

In Vivo Bypass Efficiencies and Mutational Signatures of the Guanine Oxidation Products 2-Aminoimidazolone and 5-Guanidino-4-nitroimidazole*

Received for publication, June 24, 2004, and in revised form, August 4, 2004
Published, JBC Papers in Press, August 6, 2004, DOI 10.1074/jbc.M407117200

William L. Neeley, James C. Delaney, Paul T. Henderson‡, and John M. Essigmann§

From the Department of Chemistry and Biological Engineering Division, Massachusetts Institute of Technology, Cambridge, Massachusetts 02139

The *in vivo* mutagenic properties of 2-aminoimidazolone and 5-guanidino-4-nitroimidazole, two products of peroxynitrite oxidation of guanine, are reported. Two oligodeoxynucleotides of identical sequence, but containing either 2-aminoimidazolone or 5-guanidino-4-nitroimidazole at a specific site, were ligated into single-stranded M13mp7L2 bacteriophage genomes. Wild-type AB1157 *Escherichia coli* cells were transformed with the site-specific 2-aminoimidazolone- and 5-guanidino-4-nitroimidazole-containing genomes, and analysis of the resulting progeny phage allowed determination of the *in vivo* bypass efficiencies and mutational signatures of the DNA lesions. 2-Aminoimidazolone was efficiently bypassed and 91% mutagenic, producing almost exclusively G to C transversion mutations. In contrast, 5-guanidino-4-nitroimidazole was a strong block to replication and 50% mutagenic, generating G to A, G to T, and to a lesser extent, G to C mutations. The G to A mutation elicited by 5-guanidino-4-nitroimidazole implicates this lesion as a novel source of peroxynitrite-induced transition mutations *in vivo*. For comparison, the error-prone bypass DNA polymerases were overexpressed in the cells by irradiation with UV light (SOS induction) prior to transformation. SOS induction caused little change in the efficiency of DNA polymerase bypass of 2-aminoimidazolone; however, bypass of 5-guanidino-4-nitroimidazole increased nearly 10-fold. Importantly, the mutation frequencies of both lesions decreased during replication in SOS-induced cells. These data suggest that 2-aminoimidazolone and 5-guanidino-4-nitroimidazole in DNA are substrates for one or more of the SOS-induced Y-family DNA polymerases and demonstrate that 2-aminoimidazolone and 5-guanidino-4-nitroimidazole are potent sources of mutations *in vivo*.

Oxidative damage of DNA is implicated as a cause of aging (1–3), carcinogenesis (4–6), and a variety of noncancerous diseases such as Alzheimer disease and cardiovascular disease (7) and in the progression to acquired immunodeficiency syndrome in human immunodeficiency virus-infected patients (8). The reactive species responsible for DNA damage are generated by

common endogenous processes (9) such as respiration and inflammation (10, 11). During inflammation, an assortment of reactive oxygen and nitrogen intermediates are generated by activated immune system cells (11), and reaction of these molecules with DNA produces dozens of oxidized nucleobase derivatives (12).

The radicals nitric oxide (NO) and superoxide (O_2^-) are produced by macrophages and neutrophils (two types of inflammatory cells) upon immune response activation (13, 14). These radicals combine in a diffusion-limited reaction to form peroxynitrite ($ONOO^-$)¹ (15), a powerful oxidizing and nitrating agent capable of damaging a variety of biomolecules (16–18), including DNA (19). Under physiological conditions, $ONOO^-$ rapidly combines with CO_2 to form nitrosoperoxycarbonate ($ONOCO_2^-$), which subsequently undergoes homolysis to produce carbonate radical (CO_3^-) and nitrogen dioxide (NO_2) (20–22). These radicals are believed to be responsible for the oxidation and nitration of DNA caused by exposure to $ONOO^-$ (23–25).

Because guanine possesses the lowest redox potential of the four DNA nucleobases ($E_7 = 1.27$ V versus normal hydrogen electrode) (26), it is preferentially oxidized by $ONOO^-$ compared with the other natural nucleobases (27). Several products are formed directly from guanine residues in DNA including 7,8-dihydro-8-oxoguanine (8-oxoG), 8-nitroguanine (8- NO_2 -G), 2-aminoimidazolone (Iz), and 5-guanidino-4-nitroimidazole (NI) (Fig. 1) (28). The lesions 8-oxoG and 8- NO_2 -G are highly susceptible to further oxidation (27) and yield a variety of additional products (29, 30). Although many of these guanine-derived oxidation products have been characterized for their *in vivo* mutagenic potential (31, 32), Iz and NI have received little attention. To assess the biological significance and consequences of oxidatively damaged DNA, it is essential that these lesions be characterized for their genotoxic and mutagenic potential.

In the work presented here, we report the *in vivo* genotoxic and mutagenic properties of Iz and NI. Oligodeoxynucleotides (ODNs), site-specifically modified with Iz or NI, were synthesized using a method described previously (33) and a procedure developed in our laboratory (34). The biological impact of

* This work was supported by National Institutes of Health Grants CA26731 and CA080024 and by National Science Foundation Grants DBI-9729592 and CHE-9808061. The costs of publication of this article were defrayed in part by the payment of page charges. This article must therefore be hereby marked "advertisement" in accordance with 18 U.S.C. Section 1734 solely to indicate this fact.

‡ Present address: Lawrence Livermore National Laboratory, Biology and Biotechnology Research Program, L-441, Livermore, CA 94551.

§ To whom correspondence should be addressed. Tel.: 617-253-6227; Fax: 617-253-5445; E-mail: jessig@mit.edu.

¹ The abbreviations used are: $ONOO^-$, peroxynitrite; 8-oxoG, 7,8-dihydro-8-oxoguanine; Iz, 2-aminoimidazolone; NI, 5-guanidino-4-nitroimidazole; ODN, oligodeoxynucleotide; THF, tetrahydrofuran; X-gal, 5-bromo-4-chloro-3-indolyl- β -D-galactopyranoside; REAP, restriction endonuclease and post-labeling analysis of mutation frequency; WT, wild type; pol I, DNA polymerase I; Kf, Klenow fragment of DNA polymerase I; Kf (exo⁻), Klenow fragment of DNA polymerase I without exonuclease activity; pol α , calf thymus polymerase α ; pol β , human polymerase β ; pol II, DNA polymerase II; pol IV, DNA polymerase IV; pol V, DNA polymerase V; HPLC, high pressure liquid chromatography; MALDI-TOF, matrix-assisted laser desorption ionization time-of-flight.

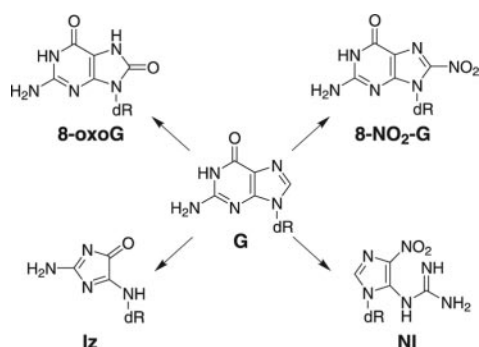


FIG. 1. Primary products of ONOO^- oxidation and nitration of guanine.

unique Iz and NI lesions was addressed under normal and SOS-induced conditions in wild-type AB1157 *Escherichia coli* cells using viral vectors containing the modified ODNs. Both lesions were bypassed by the *E. coli* replication machinery and were substrates for SOS-induced error-prone DNA polymerase bypass. Furthermore, each lesion was potentially mutagenic during DNA replication.

EXPERIMENTAL PROCEDURES

Oligodeoxynucleotides—DNA synthesis reagents were purchased from Glen Research. Unmodified ODNs were purchased from IDT, Inc. and were purified by PAGE. The 19-mer ODN sequence used was 5'-GCG AAG ACC GXG GCG TCC G-3', where X is G, Iz, NI, or a tetrahydrofuran (THF) abasic site. The 19-mer containing the THF abasic site analog was prepared as described (31).

The 19-mer containing Iz was prepared as described previously (33). Briefly, 8-methoxy-2'-deoxyguanosine was incorporated into the 19-mer ODN by the phosphoramidite method, and the ODN was deprotected and cleaved from the solid support with concentrated NH_4OH at 55 °C for 15 h. The 8-methoxy-2'-deoxyguanosine-containing ODN was purified by PAGE, and the 8-methoxy-2'-deoxyguanosine was subsequently converted to Iz by photoirradiation with 365 nm light in the presence of riboflavin. The Iz-containing 19-mer was purified by anion exchange HPLC on a Dionex NucleoPac PA-100 (4 × 250 mm) analytical column using 10% CH_3CN in water (solvent A) and aqueous 1.5 M NH_4OAc (solvent B) as solvents. A flow rate of 1.0 ml/min was used, and solvent B was increased from 10 to 25% over 2.5 min and then increased from 25 to 100% over 30 min. The purified 19-mer was characterized using MALDI-TOF mass spectrometry (calculated M_r , 5824.8; found M_r , 5825.8) and enzymatic digestion to nucleosides followed by HPLC analysis. For the enzymatic digestion, 50 mM Tris-Cl, pH 7.0, 0.1 mM ZnSO_4 , 18 units of nuclease P1, 12 units of alkaline phosphatase (both enzymes from Roche Applied Science), and 2 nmol of Iz-containing 19-mer in 50 μl were incubated at room temperature for 30 min and then immediately analyzed by HPLC. For the HPLC analysis, a Supelco Supercosil LC-18-DB (250 × 2.1 mm, 5 μm) column was used with aqueous 150 mM NH_4OAc as solvent A and CH_3CN as solvent B. A flow rate of 0.25 ml/min was used, and solvent B was increased from 0 to 15% over 40 min. Five peaks were observed with UV-visible spectra consistent with the nucleosides Iz, C, G, T, and A.

The ODN containing NI was prepared by incorporating 5-bromo-4-nitroimidazole into the 19-mer sequence by the phosphoramidite method and subsequently treating the 19-mer with 0.5 M guanidine in THF and then with concentrated NH_4OH to produce the 19-mer containing NI (34). The NI-containing 19-mer was purified by C18 reversed phase HPLC (34) and by anion exchange HPLC as described above and characterized using MALDI-TOF mass spectrometry (calculated M_r , 5882.9; found M_r , 5882.7) and enzymatic digestion with snake venom phosphodiesterase (ICN Biomedical) and alkaline phosphatase (34) followed by HPLC analysis (same method as described for the 19-mer containing Iz). For the HPLC analysis, five peaks were observed with UV-visible spectra consistent with the nucleosides NI, C, G, T, and A.

Genome Construction—Genomes were constructed in triplicate (Fig. 2) on a 10-pmol scale as described previously (31, 32, 35). Briefly, the single-stranded M13 DNA was linearized by cleavage with EcoRI (30 units/pmol DNA, 23 °C for 8 h) at a hairpin containing a single EcoRI site (35). The genome was recircularized by annealing in the presence of the 5'-phosphorylated 19-mer insert and two "scaffold" ODNs (sequences that are partially complementary to the 5' and 3' sides of the

insert and the genomic DNA termini) and incubating with 22.5 units/ μl T4 DNA ligase (New England Biolabs) for 2 h at 16 °C in a volume of 55 μl (31). Two short scaffolds are used to leave a single-stranded gap at the site of the lesion, thereby facilitating efficient ligation regardless of the lesion structure. The scaffold DNA was removed using the exonuclease activity of T4 DNA polymerase (Amersham Biosciences) by treating with 0.25 units/ μl for 1 h at 16 °C in a volume of 65 μl (36, 37). Under these conditions, scaffold digestion was complete as determined by using a radiolabeled scaffold and analyzing the reaction with PAGE and phosphorimaging. The genome constructs were diluted to 115 μl with H_2O , extracted with 100 μl of phenol:chloroform:isoamyl alcohol (25:24:1) (Invitrogen) and desalted with Sephadex G50 fine resin (Amersham Biosciences).

The stability of the lesion-containing 19-mers was assessed using MALDI-TOF mass spectrometry. The 19-mers were exposed to the conditions used for genome construction with the exception that M13 DNA, other ODNs, and enzymes were excluded. The mass spectra of the 19-mers were essentially unchanged after exposure to the mock genome construction conditions.

The amount of circular, 19-mer insert-containing genome in each sample was quantified by agarose gel electrophoresis and phosphorimaging. This was accomplished by annealing 1 pmol of a 5' ^{32}P -labeled 30-mer probe ODN (5'-TCC CAG TCA CGA CGT TGT AAA ACG ACG GCC-3') to 0.1 pmol of each genome construct in a region of the genome that did not include the lesion-containing 19-mer insert. The annealing solution consisted of 100 mM NaCl, 4.2% Ficoll, 0.042% bromophenol blue, and 0.042% xylene cyanol FF in a volume of 15.5 μl . The genome-probe mixtures (15.5 μl) were run on a 0.9% agarose gel in 1× Tris borate/EDTA buffer for 4 h at 100 V, after which the free probe front was excised. The gel was run for an additional 3 h and then transferred onto a glass plate and dried under a box fan for 36 h. The amount of circular genome was quantified by phosphorimaging and the genome construct solution volumes adjusted such that each solution used for cell transformation contained an equal concentration of circular DNA.

Preparation of Electrocompetent Cells—Two 150-ml aliquots of LB medium were each inoculated with 1.5 ml from separate overnight cultures of wild-type AB1157 *E. coli* and grown on a shaker at 37 °C to an A_{600} of ~0.4. Each culture was centrifuged, resuspended in 25 ml of 10 mM MgSO_4 , and transferred to a large (150 × 15 mm) Petri dish. The SOS system was induced in the cells by irradiating with 254 nm light (45 J/m^2 of energy), immediately transferring the cells to two 125-ml aliquots of 2× YT medium, and growing them for 40 min at 37 °C with shaking. Uninduced cells were treated identically, except without exposure to UV light. The 2× YT cultures were centrifuged, combined, and washed twice with 175 ml of deionized water. The electrocompetent cells were resuspended in 4 ml of a 10% solution of glycerol in water, stored at 4 °C, and used the following day.

Translesion Bypass Efficiency—An equal amount of each circular genome construct was mixed with 0.025 pmol of internal standard (wild-type circular single-stranded M13mp7L2 DNA) and 100 μl of electrocompetent cells. The cell/genome mixtures were electroporated and transferred to 10 ml of LB, generating at least 10^5 independent transformed cells as determined by plating of an aliquot onto agar plates. The cultures were incubated at room temperature for at least 30 min and then incubated on a roller drum for 4 h at 37 °C to amplify the progeny phage. The cells were spun down and the progeny phage-containing supernatant retained. In this system, successful replication of the genomes by the *E. coli* host leads to the production of progeny phage. When plated on a lawn of NR9050 indicator *E. coli* in the presence of isopropyl 1-thio- β -D-galactopyranoside and X-gal (Gold Biotechnology), progeny phage derived from genomes containing the 19-mer insert produce blue plaques if no mutation, a point mutation, or an in-frame insertion or deletion mutation occurs at the lesion site, whereas progeny phage from WT M13mp7L2 genomes, genomes lacking an insert (genetic engineering mutants), and lesion-induced out-of-frame insertions and deletions produce clear plaques (31). Thus, the amplified progeny phage were diluted and plated such that ~1000–2000 total plaques were produced per Petri dish, and the number of blue and clear plaques per plate was counted. The number of normalized blue plaques resulting from each lesion-containing genome relative to that of the normalized guanine control indicated the bypass efficiency of a lesion (see "Results" for details). The normalization allowed direct comparison of lesion bypass by DNA polymerase(s) between genomes containing different inserts, regardless of unavoidable variation in factors such as electroporation efficiency and the total number of plaques on each plate.

Mutation Type and Frequency—Electrocompetent cells were transformed with each genome construct, as described in the previous sec-

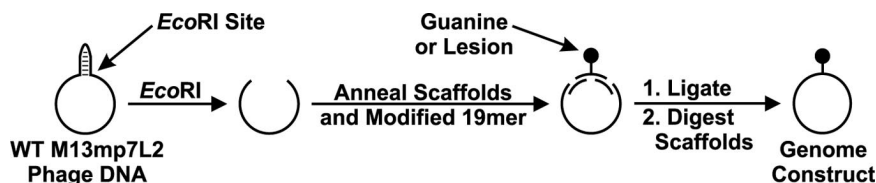


FIG. 2. Construction of genomes containing a guanine residue or DNA lesion at a specific site. A 5'-phosphorylated 19-mer oligodeoxynucleotide insert containing a guanine residue or DNA lesion at a specific site (denoted by a solid circle) is positioned within a single-stranded WT M13mp7L2 bacteriophage genome using two DNA scaffolds. The 19-mer insert is ligated into the genome using T4 DNA ligase, and the scaffolds are digested using the exonuclease activity of T4 DNA polymerase to produce the genome construct.

tion, except that the internal standard was excluded. As before, the electroporations produced at least 10^5 independent transformed cells. Amplified progeny phage (100 μ l) and 10 μ l of an overnight growth of SCS110 *E. coli* were added to 10 ml of LB medium and grown for 6 h at 37 °C on a roller drum. The cultures were centrifuged, and the phage-containing supernatant was retained. Single-stranded phage DNA was isolated from 700 μ l of each sample using a QIAprep Spin M13 kit (Qiagen). The region containing the lesion site was amplified by PCR as described previously (31), except 0.7 μ M of each primer was used, and the resultant 101-mer PCR product was purified using a QIAprep PCR purification kit (Qiagen). The restriction endonuclease and post-labeling analysis of mutation frequency (REAP) assay was used to determine the identity of the base at the site formerly occupied by the lesion (31, 32, 35, 38).

RESULTS

Genome Construction—Convertible nucleoside phosphoramidites were used to introduce each oxidized DNA lesion into a 19-mer ODN at a defined site. Following incorporation into the 19-mer by automated DNA synthesis, 8-methoxyguanine was converted to Iz by photoirradiation in the presence of riboflavin (33). Using a procedure recently developed in our laboratory, NI was formed within an ODN from the convertible nucleoside 5-bromo-4-nitroimidazole by treatment of the ODN with guanidine (34). Each ODN was characterized by MALDI-TOF mass spectrometry and by nuclease and phosphatase digestion followed by HPLC analysis. Single-stranded M13mp7L2 viral genomes containing Iz or NI at a specific site in the genome were constructed as shown in Fig. 2. An aliquot of each genome construct, annealed to a radiolabeled ODN probe, was analyzed by agarose gel electrophoresis and phosphorimaging to assess the yield of circular insert-containing genome. Following quantification, the genome construct solutions were normalized such that each contained an equivalent amount of circular insert-containing genome. The stability of each lesion to the genome construction conditions was confirmed by MALDI-TOF mass spectrometry after subjecting the lesion-containing ODNs to the same conditions.

Translesion Bypass Efficiency—A viral plaque assay based on *lacZ* α -complementation was employed for the determination of the lesion bypass efficiency (Fig. 3). In this system, phage produced from genomes containing the 19-mer insert cause the formation of blue plaques when plated on isopropyl 1-thio- β -D-galactopyranoside/X-gal indicator plates if either no mutation or a point mutation occurs at the lesion site, and phage produced from WT M13mp7L2 genomes produce clear plaques. The number of phage that form blue plaques varies with the efficiency of lesion bypass, and the rate of replication of the WT M13mp7L2 genomes is assumed to be independent of the identity of the insert-containing genomes. Thus, a genome containing a lesion that partially blocks replication yields a lower proportion of progeny phage relative to a genome containing a freely bypassed lesion. Because the same amount of internal standard (WT M13mp7L2 genome) was used in each mixture, the blue to clear ratio of each mixture can be directly compared after being normalized to reflect the identical amount of internal standard in each mixture. The bypass efficiency of a lesion is scaled relative to guanine, which is defined

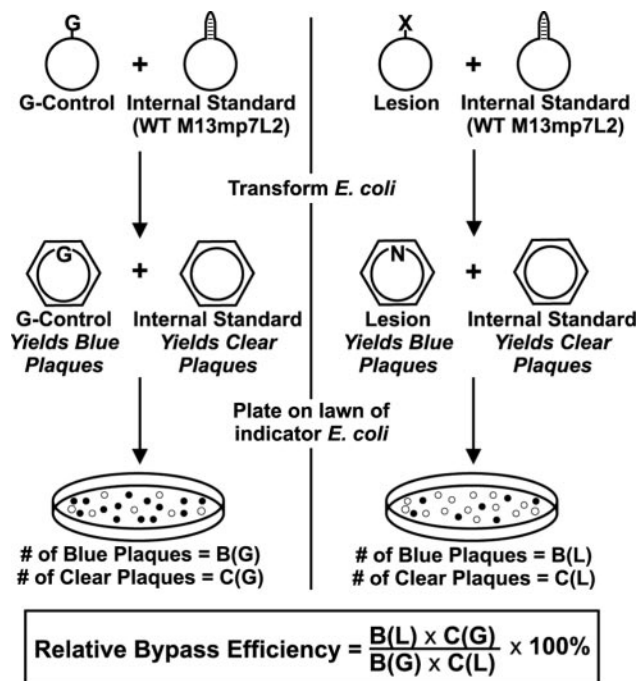


FIG. 3. Assay for determining the efficiency of DNA polymerase bypass of a DNA lesion. Genome constructs containing a site-specific guanine residue (G) or DNA lesion (X) are separately mixed with a known amount of internal standard (single-stranded WT M13mp7L2 genome), and the equally proportioned mixtures are used to transform *E. coli* cells. Progeny phage (denoted by a circle with a hexagon) derived from a genome construct have a functional *lacZ* gene, whereas phage containing the WT M13mp7L2 genome do not. Thus, the composition of the progeny phage mixtures can be assayed by plating on a lawn of NR9050 indicator *E. coli* in the presence of isopropyl 1-thio- β -D-galactopyranoside and X-gal and counting the number of blue and clear plaques produced by the phage infections.

as having a bypass efficiency of 100%. From this logic the equation given in Fig. 3 results, where the term $B(L)/B(G)$ is the definition of relative bypass efficiency and the term $C(G)/C(L)$ is the normalization factor. A limitation of this assay is that lesion-induced out-of-frame insertion and deletion mutations would also produce clear plaques and therefore not be counted as bypass events. However, as discussed in the next section the lesions studied here induced negligible amounts of observable insertion and deletion mutations and so a correction for these events was not performed.

In normal WT AB1157 *E. coli*, the bypass efficiency of Iz was $60 \pm 5\%$ (Fig. 4). By contrast, NI was a much stronger replication block and was bypassed with an efficiency of only $7.0 \pm 1.6\%$. As a control, we also determined the bypass efficiency of a synthetic THF abasic site. The THF lesion was bypassed with an efficiency of $5.8 \pm 0.7\%$ in agreement with previous work showing that this lesion is a block to DNA replication (31, 32, 39). The bypass efficiencies of the lesions were also determined in cells with the SOS system induced. Under these conditions, the bypass efficiency of Iz did not change significantly ($71 \pm$

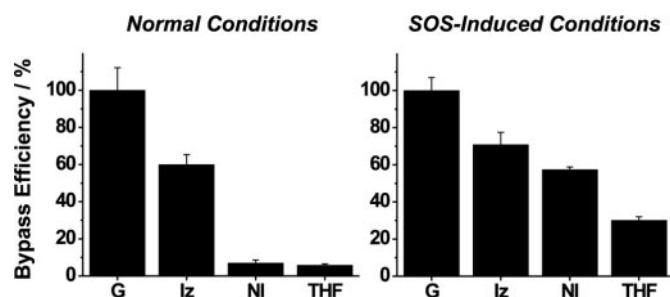


FIG. 4. Bypass efficiency of Iz, NI, and a THF abasic site relative to G. The results shown are the average of three experiments, with the experimental error given as a 95% confidence interval of the mean.

7%); however, the bypass efficiency of NI increased a remarkable 8-fold to $57 \pm 1\%$. The bypass efficiency of the THF lesion increased to $30 \pm 2\%$, demonstrating that the SOS system was indeed induced.

Mutation Type and Frequency—The mutational signature of each lesion in WT AB1157 *E. coli* was determined using the REAP assay (Fig. 5). Insertion and deletion mutations that do not compromise the BbsI recognition site or the PCR primer sites are detectable by the REAP assay during the PAGE purification step and were negligible in this work (less than 1%, data not shown).

In normal cells, the mutation frequency of Iz was 91% versus 50% for NI (Fig. 6). The mutations induced by Iz were essentially all G→C mutations, as predicted by molecular orbital calculations and *in vitro* primer extension experiments (40, 41). NI caused $8.9 \pm 0.5\%$ G→C mutations and a roughly equivalent amount of G→A and G→T mutations ($19 \pm 2\%$ and $22 \pm 3\%$, respectively). The mutation type and frequency for each lesion was also determined in SOS-induced cells to investigate the effect of the SOS response system on the coding properties of these lesions. Interestingly, Iz and NI had somewhat lower overall mutation frequencies of 84 and 33%, respectively. The coding properties of Iz were more degenerate under SOS-induced conditions. Whereas Iz caused $2.0 \pm 0.1\%$ G→A and $1.1 \pm 0.2\%$ G→T mutations without SOS induced, the lesion now induced $3.4 \pm 0.5\%$ G→A and $5.5 \pm 0.8\%$ G→T mutations. The mutational signature of NI also differed in SOS-induced cells, as the lesion induced many fewer G→A and G→C mutations ($13 \pm 2\%$ and $2.5 \pm 0.6\%$, respectively).

DISCUSSION

To assess the biological fate of Iz and NI in DNA, we have determined the relative bypass efficiency and the mutation type and frequency of each lesion *in vivo*. The Iz derivative is a major and ubiquitous *in vitro* product of guanine oxidation. In addition to forming as a result of ONOO⁻ oxidation (28), this lesion also forms when guanine is oxidized by other reactants including hydroxyl radical (42), Mn-TMPyp/KHSO₅ (a chemical nuclease) (43–45), and riboflavin (photooxidation) (40–42, 46). Direct formation of Iz from 8-oxoG has also been observed (40, 47). On a biological time scale, Iz is stable ($t_{1/2}$ in single-stranded DNA ~16 h at 37 °C) (33) but can hydrolyze to form an oxazolone derivative. Oxazolone is bypassed efficiently and exhibits a mutation frequency similar to that of Iz *in vivo* (86%) but preferentially generates G→T transversion mutations (31). In distinct contrast, NI has been observed only as a result of ONOO⁻-related chemistry (28, 48, 49). NI is a chemically stable lesion (when heated to 90 °C for 6 h at pH 7, ~10–15% decomposition of an ODN containing NI occurs) (49) and is refractory to repair by Fpg glycosylase (*MutM*) and endonuclease III *in vitro* (48). The chemical and biological properties of NI make this lesion a potential biomarker of ONOO⁻-mediated oxidation of DNA (28, 48).

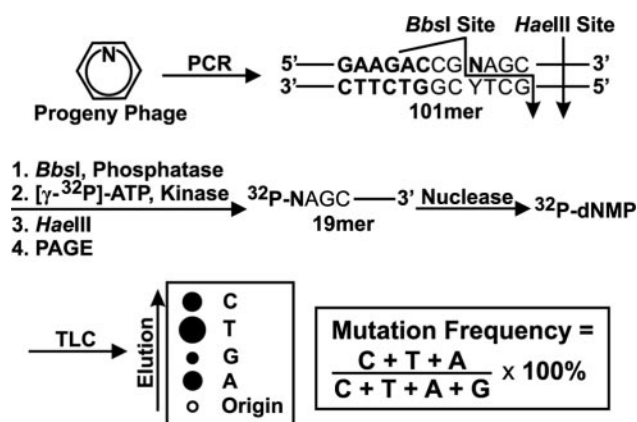


FIG. 5. REAP assay for determining the mutation type and frequency of a DNA lesion. *E. coli* cells are transformed with genome constructs site-specifically modified with a guanine residue or DNA lesion. Position N in the resultant progeny phage genomes represents the site formerly occupied by the site-specific modification. The region containing N is PCR amplified to yield a 101-mer containing BbsI and HaeIII recognition sites. The BbsI digestion product is radiolabeled and digested with HaeIII to produce a 19-mer with N radiolabeled. PAGE purification of the 19-mer also allows insertion and deletion mutations (appearing as ODNs of longer or shorter length than the 19-mer) to be quantified, if present. Digestion of the 19-mer with nuclease P1 and subsequent partitioning of the nucleotide mixture by TLC allows the point mutation type and frequency to be quantified using phosphorimaging.

In vitro studies have been conducted with Iz and NI, and the results suggest they would be both replication blocks and mutagenic *in vivo*. *Ab initio* studies of Iz *in vacuo* and using a self-consistent reaction field method of solvation indicate that this lesion should give G→C mutations because of its apparent ability to mimic the hydrogen-bonding face of C and to form a stable base pair with G (40, 41). Replication of the lesion using DNA polymerase I (pol I), and the Klenow fragment of pol I (Kf), showed that the lesion indeed codes exclusively as a cytosine, but is inefficiently bypassed (40). In contrast, the site-specific bacteriophage replication experiments presented here showed that the lesion was bypassed relatively efficiently and had a mutation frequency of 91%, suggesting one or more polymerases in addition to pol I may be responsible for the bypass of Iz under normal conditions.

The bypass and coding properties of DNA containing NI were studied previously using the purified DNA polymerases Kf (exo⁻), calf thymus polymerase α (pol α), and human polymerase β (pol β) (48). All three polymerases could insert a nucleotide opposite the lesion, and although a kinetic analysis was not performed, the data suggested that extension of the NI-containing base pair by Kf (exo⁻) and pol α is rate-limiting and results in poor translesion synthesis. The nucleotides A and G were incorporated opposite NI by Kf (exo⁻) and pol α , with Kf (exo⁻) favoring insertion of C opposite the lesion. Interestingly, pol β efficiently bypassed the lesion and incorporated mostly C, rendering the lesion non-toxic and non-mutagenic. Our results differ from the *in vitro* data because substantial amounts of T were incorporated opposite NI, thereby producing G→A mutations *in vivo*. This observation indicates pol I is probably not solely responsible for the bypass of NI because this polymerase did not incorporate T opposite the lesion *in vitro*. The bypass efficiency of NI in WT cells shows that NI is a significant block to replication and has a bypass efficiency similar to that of the THF synthetic abasic site. This observation correlates with our recent thermal melting study that showed NI greatly destabilizes duplex DNA regardless of the identity of the base paired opposite the lesion. To explain this observation, we proposed that NI adopts a nonplanar and potentially DNA-distorting

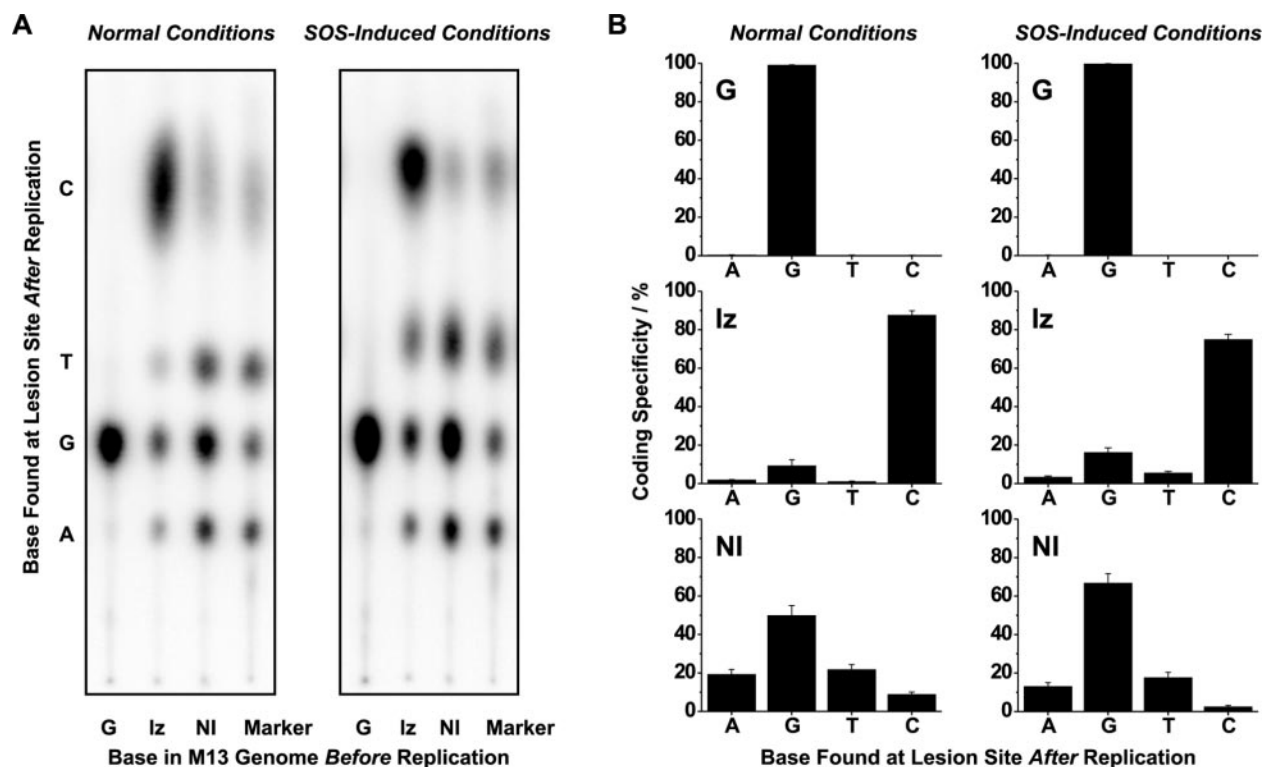


FIG. 6. REAP assay results for G, Iz, and NI. A, representative polyethyleneimine TLC analysis of point mutation type and frequency. B, quantification of the TLC data for G (top), Iz (center), and NI (bottom). The graphical data shown are the average of three experiments, with the experimental error given as a 95% confidence interval of the mean.

conformation (34). Thus, the low bypass efficiency of NI may result from the inability of NI to fit within the tight active site of a replicative DNA polymerase (50). Alternatively, the large increase in NI bypass efficiency when replicated in SOS-induced cells may indicate the involvement of Y-family DNA lesion bypass polymerases, which have less sterically restrictive active sites and can bypass numerous types of lesions (51–58).

The differences in bypass efficiency and coding specificity of the lesions in normal *versus* SOS-induced cells indicate that SOS-induced proteins contribute to the processing of these lesions. In normal cells, the number of SOS-inducible DNA polymerase molecules per cell is ~50 for pol II (59), 250 for pol IV (60), and fewer than 15 for pol V (61). Upon SOS induction, the number of DNA polymerase molecules per cell increases to about 350 for pol II (59), 2500 for pol IV (60), and 200 for pol V (61). It has been demonstrated that one or more of these polymerases are required to bypass certain DNA lesions, and the specific polymerases involved vary depending on the sequence context in which the lesion resides (62–64). Experiments using polymerase-deficient cell lines would address which of the SOS-induced polymerases are involved in the bypass of Iz and NI.

The mutational signatures of Iz and NI determined here using site-specifically modified genomes correlate well with previous cell-based mutagenesis studies (19, 25). In one report, a pSP189 shuttle vector containing the *supF* gene was treated with ONOO⁻ in the presence of NaHCO₃ (a physiological buffer component that facilitates the reaction of ONOO⁻ with DNA by supplying CO₂) followed by replication in MBL50 *E. coli* (25). Essentially all mutations occurred at G-C base pairs and consisted of 55% G→C, 31% G→T, and 11% G→A mutations. We previously showed *in vivo* that the 8-oxoG secondary oxidation products cyanuric acid, oxaluric acid, and oxazolone give exclusively G→T mutations (31), whereas guanidinohydantoin generates exclusively G→C mutations and the spiroiminodihydantoin diastereomers yield a mixture of G→C and G→T

mutations (32). In both studies, 8-oxoG was slightly mutagenic and induced only G→T mutations, so the discovery that guanidinohydantoin and the spiroiminodihydantoin diastereomers generate G→C mutations implicated these lesions as the possible sources of the *in vivo* G→C mutations found in the *supF*/pSP189 system. The results in the present work implicate Iz as an additional *in vivo* source of G→C mutations. Importantly, prior to this work no ONOO⁻-derived lesions had been found to give significant amounts of G→A mutations. Our results implicate NI as a possible source of the G→A mutations observed during the *supF*/pSP189 study.

Iz and NI are formed directly from guanine upon oxidation by ONOO⁻. When replicated *in vivo*, these lesions are bypassed and potentially mutagenic, collectively inducing G→C, G→T, and G→A mutations. Our results support a role for Iz and NI as contributors to the mutational spectrum observed when ONOO⁻-treated DNA is replicated *in vivo*. If these lesions persist in cells, they may be powerful sources of mutations.

Acknowledgments—We thank Dr. Yuriy O. Alekseyev for helpful discussions. We also acknowledge the MIT Biological Engineering Division Mass Spectrometry Laboratory and the Department of Chemistry Instrumentation Facility.

REFERENCES

- Sastre, J., Pallardo, F. V., and Vina, J. (2003) *Free Radic. Biol. Med.* **35**, 1–8
- Finkel, T., and Holbrook, N. J. (2000) *Nature* **408**, 239–247
- Mandavilli, B. S., Santos, J. H., and Van Houten, B. (2002) *Mutat. Res.* **509**, 127–151
- Klaunig, J. E., and Kamendulis, L. M. (2004) *Annu. Rev. Pharmacol. Toxicol.* **44**, 239–267
- Hussain, S. P., Hofseth, L. J., and Harris, C. C. (2003) *Nat. Rev. Cancer* **3**, 276–285
- Olinski, R., Gackowski, D., Foksinski, M., Rozalski, R., Roszkowski, K., and Jaruga, P. (2002) *Free Radic. Biol. Med.* **33**, 192–200
- Cooke, M. S., Evans, M. D., Dizdaroglu, M., and Lunec, J. (2003) *FASEB J.* **17**, 1195–1214
- Jaruga, P., Jaruga, B., Gackowski, D., Oleczak, A., Halota, W., Pawlowska, M., and Olinski, R. (2002) *Free Radic. Biol. Med.* **32**, 414–420
- De Bont, R., and Van Larebeke, N. (2004) *Mutagenesis* **19**, 169–185
- Turrens, J. F. (1997) *Biosci. Rep.* **17**, 3–8
- Ohshima, H., Tatemichi, M., and Sawa, T. (2003) *Arch. Biochem. Biophys.* **417**,

3-11

12. Bjelland, S., and Seeberg, E. (2003) *Mutat. Res.* **531**, 37-80
13. Xia, Y., and Zweier, J. L. (1997) *Proc. Natl. Acad. Sci. U. S. A.* **94**, 6954-6958
14. Carreras, M. C., Pargament, G. A., Catz, S. D., Poderoso, J. J., and Boveris, A. (1994) *FEBS Lett.* **341**, 65-68
15. Burney, S., Caulfield, J. L., Niles, J. C., Wishnok, J. S., and Tannenbaum, S. R. (1999) *Mutat. Res.* **424**, 37-49
16. Radi, R., Beckman, J. S., Bush, K. M., and Freeman, B. A. (1991) *J. Biol. Chem.* **266**, 4244-4250
17. Radi, R., Beckman, J. S., Bush, K. M., and Freeman, B. A. (1991) *Arch. Biochem. Biophys.* **288**, 481-487
18. Pryor, W. A., Jin, X., and Squadrito, G. L. (1994) *Proc. Natl. Acad. Sci. U. S. A.* **91**, 11173-11177
19. Juedes, M. J., and Wogan, G. N. (1996) *Mutat. Res.* **349**, 51-61
20. Lymar, S. V., and Hurst, J. K. (1996) *Chem. Res. Toxicol.* **9**, 845-850
21. Lymar, S. V., and Hurst, J. K. (1995) *J. Am. Chem. Soc.* **117**, 8867-8868
22. Lymar, S. V., and Hurst, J. K. (1998) *Chem. Res. Toxicol.* **11**, 714-715
23. Shafirovich, V., Dourandian, A., Huang, W., and Geacintov, N. E. (2001) *J. Biol. Chem.* **276**, 24621-24626
24. Dedon, P. C., and Tannenbaum, S. R. (2004) *Arch. Biochem. Biophys.* **423**, 12-22
25. Pamir, B., and Wogan, G. N. (2003) *Chem. Res. Toxicol.* **16**, 487-492
26. Steenken, S., and Jovanovic, S. V. (1997) *J. Am. Chem. Soc.* **119**, 617-618
27. Burney, S., Niles, J. C., Dedon, P. C., and Tannenbaum, S. R. (1999) *Chem. Res. Toxicol.* **12**, 513-520
28. Niles, J. C., Wishnok, J. S., and Tannenbaum, S. R. (2001) *J. Am. Chem. Soc.* **123**, 12147-12151
29. Lee, J. M., Niles, J. C., Wishnok, J. S., and Tannenbaum, S. R. (2002) *Chem. Res. Toxicol.* **15**, 7-14
30. Tretyakova, N. Y., Niles, J. C., Burney, S., Wishnok, J. S., and Tannenbaum, S. R. (1999) *Chem. Res. Toxicol.* **12**, 459-466
31. Henderson, P. T., Delaney, J. C., Gu, F., Tannenbaum, S. R., and Essigmann, J. M. (2002) *Biochemistry* **41**, 914-921
32. Henderson, P. T., Delaney, J. C., Muller, J. G., Neeley, W. L., Tannenbaum, S. R., Burrows, C. J., and Essigmann, J. M. (2003) *Biochemistry* **42**, 9257-9262
33. Ikeda, H., and Saito, I. (1999) *J. Am. Chem. Soc.* **121**, 10836-10837
34. Neeley, W. L., Henderson, P. T., and Essigmann, J. M. (2004) *Org. Lett.* **6**, 245-248
35. Delaney, J. C., and Essigmann, J. M. (1999) *Chem. Biol.* **6**, 743-753
36. Moriya, M. (1993) *Proc. Natl. Acad. Sci. U. S. A.* **90**, 1122-1126
37. Moriya, M., Zhang, W., Johnson, F., and Grollman, A. P. (1994) *Proc. Natl. Acad. Sci. U. S. A.* **91**, 11899-11903
38. Kroeger, K. M., Jiang, Y. L., Kow, Y. W., Goodman, M. F., and Greenberg, M. M. (2004) *Biochemistry* **43**, 6723-6733
39. Reuven, N. B., Tomer, G., and Livneh, Z. (1998) *Mol. Cell* **2**, 191-199
40. Kino, K., and Sugiyama, H. (2001) *Chem. Biol.* **8**, 369-378
41. Kino, K., Saito, I., and Sugiyama, H. (1998) *J. Am. Chem. Soc.* **120**, 7373-7374
42. Cadet, J., Berger, M., Buchko, G. W., Joshi, P. C., Raoul, S., and Ravanat, J. L. (1994) *J. Am. Chem. Soc.* **116**, 7403-7404
43. Vialas, C., Pratviel, G., Claparols, C., and Meunier, B. (1998) *J. Am. Chem. Soc.* **120**, 11548-11553
44. Vialas, C., Pratviel, G., Bernadou, J., and Meunier, B. (1999) *Nucleosides Nucleotides* **18**, 1061-1063
45. Vialas, C., Claparols, C., Pratviel, G., and Meunier, B. (2000) *J. Am. Chem. Soc.* **122**, 2157-2167
46. Torun, L., and Morrison, H. (2003) *Photochem. Photobiol.* **77**, 370-375
47. Luo, W., Muller, J. G., and Burrows, C. J. (2001) *Org. Lett.* **3**, 2801-2804
48. Gu, F., Stillwell, W. G., Wishnok, J. S., Shalloo, A. J., Jones, R. A., and Tannenbaum, S. R. (2002) *Biochemistry* **41**, 7508-7518
49. Joffe, A., Mock, S., Yun, B. H., Kolbanovskiy, A., Geacintov, N. E., and Shafirovich, V. (2003) *Chem. Res. Toxicol.* **16**, 966-973
50. Kool, E. T. (2002) *Annu. Rev. Biochem.* **71**, 191-219
51. Yang, W. (2003) *Curr. Opin. Struct. Biol.* **13**, 23-30
52. Ohmori, H., Friedberg, E. C., Fuchs, R. P., Goodman, M. F., Hanaoka, F., Hinkle, D., Kunkel, T. A., Lawrence, C. W., Livneh, Z., Nohmi, T., Prakash, L., Prakash, S., Todo, T., Walker, G. C., Wang, Z., and Woodgate, R. (2001) *Mol. Cell* **8**, 7-8
53. Goodman, M. F. (2002) *Annu. Rev. Biochem.* **71**, 17-50
54. Wagner, J., Gruz, P., Kim, S. R., Yamada, M., Matsui, K., Fuchs, R. P., and Nohmi, T. (1999) *Mol. Cell* **4**, 281-286
55. Tang, M., Shen, X., Frank, E. G., O'Donnell, M., Woodgate, R., and Goodman, M. F. (1999) *Proc. Natl. Acad. Sci. U. S. A.* **96**, 8919-8924
56. Shen, X., Sayer, J. M., Kroth, H., Ponten, I., O'Donnell, M., Woodgate, R., Jerina, D. M., and Goodman, M. F. (2002) *J. Biol. Chem.* **277**, 5265-5274
57. Maor-Shoshani, A., Ben Ari, V., and Livneh, Z. (2003) *Proc. Natl. Acad. Sci. U. S. A.* **100**, 14760-14765
58. Ling, H., Boudsocq, F., Woodgate, R., and Yang, W. (2001) *Cell* **107**, 91-102
59. Qiu, Z., and Goodman, M. F. (1997) *J. Biol. Chem.* **272**, 8611-8617
60. Kim, S. R., Matsui, K., Yamada, M., Gruz, P., and Nohmi, T. (2001) *Mol. Genet. Genomics* **266**, 207-215
61. Woodgate, R., and Ennis, D. G. (1991) *Mol. Gen. Genet.* **229**, 10-16
62. Napolitano, R., Janel-Bintz, R., Wagner, J., and Fuchs, R. P. (2000) *EMBO J.* **19**, 6259-6265
63. Fuchs, R. P., Koffel-Schwartz, N., Pelet, S., Janel-Bintz, R., Napolitano, R., Becherel, O. J., Broschard, T. H., Burnouf, D. Y., and Wagner, J. (2001) *Biochem. Soc. Trans.* **29**, 191-195
64. Wagner, J., Etienne, H., Janel-Bintz, R., and Fuchs, R. P. (2002) *DNA Repair (Amst.)* **1**, 159-167